Atmospheric
Chemistry
and Physics
Discussions

Open Access

Greenhouse gas network design using backward Lagrangian particle dispersion modelling – Part 1: Methodology and Australian test case

T. Ziehn[1], A. Nickless[2], P. J. Rayner[3], R. M. Law[1], G. Roff[4], and P. Fraser[1]

[1]Centre for Australian Weather and Climate Research, CSIRO Marine and Atmospheric Research, Aspendale, VIC 3195, Australia
[2]Global Change and Ecosystem Dynamics, CSIR, Pretoria, 0005, South Africa
[3]School of Earth Sciences, University of Melbourne, Melbourne, VIC 3010, Australia
[4]Centre for Australian Weather and Climate Research, Australian Bureau of Meteorology, Docklands, VIC 3008, Australia

Correspondence to: T. Ziehn (tilo.ziehn@csiro.au)

ACPD

14, 7557–7595, 2014

Greenhouse gas network design

T. Ziehn et al.

Title Page

Abstract	Introduction
Conclusions	References
Tables	Figures

◄◄   ►►

◄   ►

Back   Close

Full Screen / Esc

Printer-friendly Version

Interactive Discussion

Abstract

This paper describes the generation of optimal atmospheric measurement networks for determining carbon dioxide fluxes over Australia using inverse methods. A Lagrangian particle dispersion model is used in reverse mode together with a Bayesian inverse modelling framework to calculate the relationship between weekly surface fluxes and hourly concentration observations for the Australian continent. Meteorological driving fields are provided by the regional version of the Australian Community Climate and Earth System Simulator (ACCESS) at 12 km resolution at an hourly time scale. Prior uncertainties are derived on a weekly time scale for biosphere fluxes and fossil fuel emissions from high resolution BIOS2 model runs and from the Fossil Fuel Data Assimilation System (FFDAS), respectively. The influence from outside the modelled domain is investigated, but proves to be negligible for the network design. Existing ground based measurement stations in Australia are assessed in terms of their ability to constrain local flux estimates from the land. We find that the six stations that are currently operational are already able to reduce the uncertainties on surface flux estimates by about 30 %. A candidate list of 59 stations is generated based on logistic constraints and an incremental optimization scheme is used to extend the network of existing stations. In order to achieve an uncertainty reduction of about 50 % we need to double the number of measurement stations in Australia. Assuming equal data uncertainties for all sites, new stations would be mainly located in the northern and eastern part of the continent.

1   Introduction

Inverse modelling has been used extensively over the last two decades in carbon cycle research to estimate surface fluxes of carbon dioxide (CO_2) on multiple temporal and spatial scales (i.e. Enting and Mansbridge, 1989; Rayner et al., 1999; Rödenbeck et al., 2003; Chevallier et al., 2010), employing mainly flask and in situ data. These

Title Page

Abstract | Introduction

Conclusions | References

Tables | Figures

|◄ | ►|

◄ | ►

Back | Close

Full Screen / Esc

Printer-friendly Version

Interactive Discussion

observations include measurements from surface stations, tall towers, air planes and ships. More recently total column data (i.e. from the Total Carbon Column Observing Network (TCCON), Wunsch et al., 2011) have also been included in inversion studies (Chevallier et al., 2011). The main focus in most studies has been on deriving CO_2

5 fluxes from atmospheric CO_2 concentration observations through the inversion of an atmospheric transport model at the global scale for large land regions or a coarse grid (Peylin et al., 2013).

A global network of ground based measurement stations has been developed over the years to monitor atmospheric CO_2 concentrations. The GLOBALVIEW

10 (GLOBALVIEW-CO_2, 2008) data product, for example, consists of over 100 stations using mainly flask samples. The accuracy of a flask measurement can be achieved with high precision and the GLOBALVIEW product states uncertainties of 0.5 to 1 ppm depending on the station's location. However, flask samples are usually only provided weekly or fortnightly which results in a poor temporal resolution and sampling selected

15 for background conditions. This is partly compensated for by continuous in situ measurements which are becoming increasing available from a number of stations world wide. Nevertheless, the sampling network is still too sparse with many gaps (i.e. in the tropics) to derive CO_2 sources and sinks at a local scale due to the under-determined nature of the inverse problem (i.e. number of sites is smaller than the number of grid

20 cells) (Kaminski et al., 1999). Many inversion studies therefore focus on the estimation of fluxes for large regions of the continental or sub-continental scale. A unique solution of the inverse problem can be obtained by including prior information on the CO_2 surface fluxes, which can be derived for example from high resolution model simulations that include the terrestrial biosphere and ocean fluxes (Kaminski et al., 1999).

25 Another issue that arises from the existing network of sampling stations is that they are mainly located at remote sites away from strong sources and sinks so that they can sample clean (well mixed) air. Key stations such as Mauna Loa, Hawaii (Keeling et al., 1976) or Cape Grim, Australia provide valuable long term time series of atmospheric CO_2 concentrations which are crucial for monitoring global atmospheric trends

(Francey et al., 2013), but they are not ideally placed to detect local changes. In fact, their focus is sampling under baseline conditions, so that any influence from local land sources is minimized.

In order to derive reliable estimates of CO_2 sources and sinks at a local scale the existing network of CO_2 measurement stations needs to be extended. Network design studies focus on optimal extensions of the existing network by considering potential stations where no data are available yet. The network design is usually performed in two steps: (1) running an atmospheric transport model for a given network in inverse mode to evaluate a cost function and (2) running an optimization algorithm to minimize the cost function. The optimized network critically depends on the criteria used in the cost function and the prior knowledge usually provided in the form of a covariance matrix (Rayner, 2004).

One of the first network design studies for CO_2 was performed by Rayner et al. (1996) where they used Bayesian synthesis inversion and simulated annealing to optimize the location of atmospheric CO_2 and $\delta^{13}C$ measurements to constrain the global carbon budget. The network was optimized for the uncertainty variance in global ocean uptake using the GISS tracer transport model at a very coarse resolution (24 × 36 gridpoints). Rayner et al. (1996) also added one station at a time successively placed at every model grid point to identify the global minimum for one extra station. This is known as incremental optimization, described in detail by Patra and Maksyutov (2002), who preferred this method over simulated annealing for its computational efficiency and to provide a continuous evolution of the observation network. Patra and Maksyutov (2002) demonstrated that both methods perform equally well using a semi-Lagrangian model at the global scale with the resolution set to 2.5° × 2.5°. Flux uncertainties were calculated for 11 ocean and 11 land regions using a base network of 115 stations from the GLOBALVIEW data set and a list of 446 pre-selected potential stations. Incremental optimisation was also used by Law et al. (2004) to identify where sites are best located to minimize the uncertainties on annual mean flux estimates for 12 subregions of Australia. The inversions were performed using response functions for 116 regions

globally with the focus on Australia represented by 44 grid points which were treated as potential new locations for the network extension.

In this study we aim to improve the methodology used in Law et al. (2004) in order to assess how the existing network of CO_2 observing stations in Australia can be extended to minimize uncertainties in CO_2 flux estimates for Australia. Instead of evaluating optimal locations on a regular grid we propose a list of candidate stations. This is more efficient than treating every grid point as a potential location. It also has the advantage, that we can take existing infrastructure into account, which will consequently result in a more realistic and cost effective network extension. In contrast to many previous studies that were mainly using flask measurements from GLOBALVIEW, we consider continuous measurements at an hourly time scale for existing and potential stations. This allows us to derive CO_2 fluxes at a high spatial and temporal resolution.

This paper (Part 1) develops the generic framework for the network design and introduces the Lagrangian particle dispersion model which we run in backward mode. We then apply this concept to the Australian continent as a test case. In a first step, we evaluate the existing network of CO_2 ground based measurement stations in terms of its ability to provide reliable flux estimates. In a second step, we demonstrate how the existing network in Australia can be extended in an optimal way.

A companion paper (Part 2, Nickless et al., 2014) focuses mainly on sensitivity analysis of parameters and choices necessary for running the optimal network design and their consequences on the results. This will be demonstrated for a South-African test case, where the optimal network is created using continuous measurements from five new instruments.

2 Methodology

The network design is based on a combination of Bayesian inverse modelling methodology applied to an atmospheric transport model and the optimization of a cost function. For a given network the cost function is calculated using a particular criteria which

involves inversion to infer CO_2 surface fluxes from CO_2 concentration measurements. The optimization will then find the optimal network by minimizing the cost function through altering the given network by adding or removing new stations.

The observed concentration (c) at a particular station at a particular time can be expressed as the sum of different contributions:

$$c = c_s + c_b + c_i \tag{1}$$

where c_s is the contribution due to surface fluxes within the modelled domain, c_b the contribution from outside the region of interest (boundary inflow) and c_i is the contribution from the initial conditions. For the network design the initial conditions are neglected, because they are very well constrained by the observations and their contribution to the flux uncertainty is therefore thought to be small. The contribution from the boundaries has to be assessed and if the influence on the flux uncertainties is not negligible, then the boundary conditions have to be included in the network design process as well.

2.1 Surface flux inversion

We use a Bayesian synthesis inversion scheme (Tarantola, 1987; Enting, 2002) which allows us to infer CO_2 surface fluxes from CO_2 measurements. A simple linear expression can be used to model the relationship between the surface fluxes and concentrations:

$$c_{mod} = \mathbf{T}f \tag{2}$$

where c_{mod} is the vector of the modelled concentrations and f the vector of the (unknown) surface fluxes. $\mathbf{T}$ is the transport or sensitivity matrix which needs to be determined. At this stage we do not include any influence from outside the domain (i.e. we set $c = c_s$). If we assume a Gaussian error distribution for the surface fluxes and

concentrations we can obtain the maximum likelihood estimate for f by minimizing the cost function:

$$J(f) = \frac{1}{2}\left((c_{\text{mod}} - c)^{\mathsf{T}}C_c^{-1}(c_{\text{mod}} - c) + (f - f_0)^{\mathsf{T}}C_{f_0}^{-1}(f - f_0)\right) \qquad (3)$$

where C_c is the error covariance matrix of the observations, vector f_0 contains prior
5 flux estimates, vector f represents predicted fluxes and C_{f_0} is the prior error covariance matrix of the surface fluxes. The cost function therefore ensures that we simultaneously minimize the mismatch between modelled concentrations and measurements and the mismatch between prior flux estimates and predicted fluxes.

The solution of the optimization problem expressed through the cost function in
10 Eq. (3) provides optimal surface fluxes based on the observations provided and also posterior uncertainties for the CO_2 fluxes expressed through the posterior covariance matrix C_f. For the network design approach we are only interested in the latter of the two, because our aim is to find a network (set of observations) that minimizes the CO_2 flux uncertainties. The posterior covariance matrix can be calculated by either of the
15 two equivalent expressions (Tarantola, 1987):

$$C_f = \left(T^{\mathsf{T}}C_c^{-1}T + C_{f_0}^{-1}\right)^{-1} \qquad (4)$$

$$= C_{f_0} - C_{f_0}T^{\mathsf{T}}\left(TC_{f_0}T^{\mathsf{T}} + C_c\right)^{-1}TC_{f_0} \qquad (5)$$

As noted by Hardt and Scherbaum (1994), the calculation of the posterior flux un-
20 certainties does not depend on a particular value of the surface fluxes or concentration observations. It only depends on the transport model, the prior flux uncertainties and observational uncertainties. This has the advantage that we can evaluate potential stations for which we do not have real observations yet and without the need to generate synthetic data.

2.2 Lagrangian Particle Dispersion Model (LPDM)

The relationship between surface fluxes and atmospheric concentrations is embodied in the transport matrix **T**. A common approach in deriving **T** is to use a Lagrangian stochastic particle dispersion model. The conventional approach is to run the model in forward mode, where particles are released at the surface (source) and tracked until they have passed the measurement station (receptor), which means that all particles need to be tracked even if they do not pass through the receptor. However, if the number of sources exceeds the number of receptors then it is more efficient to run the Lagrangian model in reverse or backward mode, where the particles are released at the receptor and tracked backwards in time to any potential surface source. The source-receptor (s-r) relationship can then be used to derive the transport matrix **T**.

Here we use the Lagrangian Particle Dispersion Model (LPDM) (Uliasz, 1994) which we run in reverse mode for each potential and existing measurement station we would like to include in the network design process. Particles are released (from the known or proposed measurement height) every 20 s for a total of four weeks for different seasons of the year and the particles position is recorded in 15 min intervals. Particles that are near the surface are counted for each grid cell to determine the surface influence or sensitivity. This can be used to generate a footprint for each station, which shows the area of influence and also to calculate the s-r relationship which forms the transport matrix **T**. Here, we follow Seibert and Frank (2004) to derive the elements of that matrix.

According to Seibert and Frank (2004) the s-r relationship for a point source (one grid cell source) is given as:

$$\frac{\partial \bar{\chi}}{\partial \dot{q}_{in}} = \frac{\Delta T V_i}{\mu_{\text{tot}}} \overline{\left(\frac{c_{in}}{\rho_{in}}\right)}, \tag{6}$$

where $\bar{\chi}$ is a mass mixing ratio (receptor) and $\dot{q}_{in}$ is a mass flux density (source). The abbreviation μ_{tot} stands for the total initial mass released at the receptor in a time interval, c_{in} is the mass concentration and ρ_{in} the air density. The index in indicates

the ith grid element and the nth time interval of length ΔT. The over bar indicates temporal averaging over time interval ΔT and V_i is the volume of grid element i.

The LPDM output does not provide mass concentrations (i.e. c_{in}) for a grid cell, but the number of particles near the surface. However, the number of particles in a given grid cell is directly related to their contribution in mass. Therefore, we do not need to assign a mass to the particles, but instead we can express the mass of the particles as a function of the number of particles, and after cancelling terms the particle count can be used directly to express the source-receptor relationship in the following way:

$$N_{in} \propto c_{in} V_i \tag{7}$$

$$N_{\text{tot}} \propto \mu_{\text{tot}} \tag{8}$$

with N_{in} the number of particles in a grid element (source) at each time interval ΔT and N_{tot} the total number of particles released during a time interval. Using the number of particles instead of their mass concentration in Eq. (6), we get:

$$\frac{\partial \bar{\chi}}{\partial \dot{q}_{in}} = \frac{\Delta T}{\rho_{in}} \overline{\left(\frac{N_{in}}{N_{\text{tot}}}\right)}, \tag{9}$$

Note that our source-receptor relationship becomes now independent of the grid cell volume V_i. The density of air can be calculated as:

$$\overline{\rho_{in}} = \frac{\Delta P}{g} \tag{10}$$

where ΔP is the pressure difference in the surface layer and g is the gravity of Earth.

We also apply a conversion from mass mixing ratio to volume mixing ratio. This is simply done by multiplying with the ratio of molecular mass of air to molecular mass of carbon, which is our quantity of interest. The elements of matrix **T** are now calculated as:

$$\frac{\partial \bar{\chi}}{\partial \dot{q}_{in}} = \frac{\Delta T g}{\Delta P} \overline{\left(\frac{N_{in}}{N_{\text{tot}}}\right)} \frac{29}{12} \times 10^6, \tag{11}$$

Title Page

Abstract | Introduction

Conclusions | References

Tables | Figures

|◄ | ►|

◄ | ►

Back | Close

Full Screen / Esc

Printer-friendly Version

Interactive Discussion

with $\bar{\chi}$ expressed in ppm. For the network design we are interested in weekly fluxes of carbon divided into day and night time contributions, which reflects the way a flux inversion is usually done. This means that we have to provide the particle count N_{in} as the sum over one week (ΔT = 1 week for day and night, divided at 6 a.m. and 6 p.m.

5 Australian Eastern Time). Therefore, the mass flux density $\dot{q}_{in}$ in Eq. (11) has units of $kg\,C\,m^{-2}\,week^{-1}$ (day/night).

We set the surface layer height to 50 m which corresponds to approximately 600 Pa (ΔP). If we consider well mixed conditions, then the source-receptor relationship should be independent of the thickness of the surface layer as long as the layer is not too deep

10 (Seibert and Frank, 2004). This is further investigated in the companion paper (Nickless et al., 2014).

2.3 Influence from outside the modelled domain

The contribution from outside the modelled domain can be thought of in terms of boundary concentrations. In order to assess the influence of the boundary concentrations

15 on the observed concentrations c we need to determine the strength of the connection between the two. This can be done by calculating the Jacobian which provides the sensitivities of observed concentrations to boundary concentrations. The boundary contribution can then be written as:

$$\boldsymbol{c}_b = \mathbf{M}_B \boldsymbol{c}_B \tag{12}$$

20 where $\mathbf{M}_B$ is the Jacobian and $\boldsymbol{c}_B$ the boundary concentrations. Depending on the elements of $\mathbf{M}_B$ we might need to include the boundary conditions in the network design.

The elements of the Jacobian for the boundary conditions can be calculated by accounting for the number of particles that disappear from the model domain during the simulation. LPDM can be set up to write out the location and time when particles

25 leave the domain and one can decide on a spatial and temporal resolution (Lauvaux et al., 2012). Here, we consider four boundaries (north, south, east and west) and we

calculate the sensitivity of hourly observed concentrations to weekly boundary concentrations. In this way the Jacobian $\mathbf{M}_B$ has 32 columns (4 boundaries × 4 weeks × 2 (day/night)) and 672 rows (hourly observations over four weeks) with its elements calculated as:

$$\frac{\partial C_B}{\partial C_{tot}} = \frac{N_B}{N_{tot}} \tag{13}$$

where N_B is the number of particles leaving the domain at one of the four boundaries during one week (day/night) and N_{tot} is the total number of particles released during one hour. Ideally, we need to calculate $\mathbf{M}_B$ for each station and then use a criterion to assess whether or not the boundary conditions affect that station. Note that we are neglecting the influence of the top boundary of the domain on the observations. This is likely to be both small and homogeneous (hence indistinguishable from the initial condition).

We can use the following simple test to assess the effect of the boundary concentrations on the network design:

$$\mathbf{C}_b = \mathbf{M}_B \mathbf{C}_I \mathbf{M}_B^T \tag{14}$$

where $\mathbf{C}_I$ is the identity matrix. The diagonal elements of $\mathbf{C}_b$ provide us with the uncertainty contribution of the boundary concentrations to the estimates of the surface fluxes. If they are smaller than one, then the uncertainty contribution of the boundary concentrations can also be considered small and we do not need to include them in the network design process.

We first assessed the influence of the boundary conditions, c_B, to see whether we need to include them in the inversion. The reason for this is that if we need to include them in the inversion, then we would have to solve for the boundary concentration c_B in addition to all the surface fluxes. This not only means that the transport matrix $\mathbf{T}$ would gain 32 additional columns, but we would also need to provide prior uncertainties for the boundary concentrations. The concentrations at the boundary are usually estimated

from global circulation models, and are subject to large errors. The optimal network should seek to reduce the uncertainty of the surface fluxes, and the improvement of the tracer transport in the global circulation models should be left as a separate problem. Since it is quite challenging to provide sensible estimates for the prior uncertainties of the boundary concentrations we would like to include them only if required (i.e. if it changes the outcome of the network design).

3 Network design for Australia

For the network design we run LPDM in backward mode for each station that we would like to include in this study. We start with simulating existing ground based measurement stations and then extend this concept for potential stations as well.

3.1 Ground based measurement stations

Australia has nine established ground based measurement stations (see Fig. 1a and Table 1) run by CSIRO or the University of Wollongong. We exclude Cape Ferguson and Otway because they currently provide only flask data and we also exclude Tumbarumba because it is not operational at this time. The remaining six stations provide continuous CO_2 measurements and form our base network. From the location of the six stations (Fig. 1a) it is obvious that Australia as a whole is not very well covered since the site locations were not determined with the goal of estimating Australian CO_2 fluxes. Rather the sites comprise (a) Global Atmosphere Watch (GAW) locations, focussed on measuring baseline air, (b) TCCON locations, (c) locations of the institutions running the sites and (d) locations linked to specific projects. In order to estimate CO_2 fluxes from the terrestrial biosphere we require stations that are able to pick up the signal from local sources. For the existing network this will depend on the wind direction and we will show later to what degree the base network is already able to reduce the uncertainties on Australian CO_2 flux estimates.

In order to improve the accuracy of CO_2 flux estimates for Australia we need to add new stations to the base network. The optimal location of new stations is determined by minimising a cost function (see Sect. 3.3) which is calculated for a number of potential locations. There are several ways of setting up a list of potential stations or candidate stations. The simplest way is to assign the stations according to a regular grid. However, this might lead to a very large number of potential stations of which many may be located in inaccessible areas.

To design a more realistic and cost efficient network, we need to include logistic constraints such as the availability of supporting infrastructure in the process of setting up the candidate list. For example, one could use the location of airports or wind farms in Australia. There is also a large number of telecommunication towers along main roads which could potentially be used. Here, we use the location of the Australian Bureau of Meteorology weather watch radar stations (NRL, 2014) as potential stations. This guarantees that all stations are accessible by road and maintained. The list of all 59 potential stations can be found in Table 2 with their location shown in Fig. 1b.

3.2 Driving data and prior uncertainties

LPDM requires meteorological driving fields which are provided in this study by the regional version of the Australian Community Climate and Earth System Simulator (ACCESS-R) (NMOC, 2013) at 12 km resolution for the Australian region at an hourly time scale. Driving data include the 3-D wind field, temperature and turbulent kinetic energy (TKE) at 39 vertical levels up to 18 km in height as well as surface pressure. These fields are provided for one example month (4 weeks) for Southern Hemisphere (SH) winter (July) and summer (January).

We also need to derive prior surface flux uncertainties for Australia and an estimate of the observational uncertainties (i.e. accuracy of concentration measurements). In terms of the prior surface flux uncertainties we consider contributions from the biosphere and from fossil fuel combustion. The biosphere flux uncertainties (1σ standard deviation) are estimated using the following simple relationship (Chevallier et al., 2010):

$$\sigma_{NEP} = \min(4\,g\,C\,m^{-2}\,day^{-1}, NPP) \tag{15}$$

where NEP is the net ecosystem productivity (net carbon flux) and NPP the net primary productivity. NPP is derived for the Australian continent from BIOS2 model simulations (Haverd et al., 2013) at a daily time scale (Fig. 2a and c). BIOS2 is a modelling framework, that uses the Community Atmosphere Biosphere Land Exchange (CABLE) model (Wang et al., 2010) at 5 km resolution ($0.05° \times 0.05°$). We then aggregate the high resolution fluxes to the resolution that we use for the network design ($1.8° \times 1.8°$) and estimate the uncertainties for NEP according to Eq. (15) for each week divided into day and night time (Fig. 2b and d).

Fossil fuel uncertainties are derived from the Fossil Fuel Data Assimilation System (FFDAS) (Rayner et al., 2010; Asefi-Najafabady et al., 2014). We use ten realisations from FFDAS version II at $0.1° \times 0.1°$, aggregate them to our network design resolution and then calculate the uncertainties from the ten realisations. Due to the fact, that fossil fuel fluxes are derived on the basis of power plant locations and night lights they are very localized and vary a lot in magnitude (Fig. 3a). When we aggregate those high resolution fluxes to our $1.8° \times 1.8°$ network design resolution we "smooth out" most of the very large fluxes (Fig. 3c). Consequently, the variation between the ten realisation of the aggregated fluxes also becomes smoother which leads to only small uncertainties (Fig. 3d). As a result, fossil fuel flux uncertainties are much smaller ($< 0.3\,g\,C\,m^{-2}\,week^{-1}$) than the uncertainties from the biosphere fluxes and their influence will also be small. Figure 3b shows the uncertainties for the ten realisation based on the original $0.1° \times 0.1°$ resolution, which are much larger for individual grid cells than the uncertainties calculated for the aggregated fluxes. However, due to computational limitations we decided not to increase the resolution for the network design in this study. The influence of the spatial surface flux resolution on the outcome of the optimal network design is investigated in Part 2 (Nickless et al., 2014).

Finally, we estimate the prior error covariance matrix of the land surface fluxes as:

$$\mathbf{C}_{f_0} = \text{diag}\left(\boldsymbol{l}_f \circ (\boldsymbol{b}_{\sigma^2} + \boldsymbol{u}_{\sigma^2})\right) \tag{16}$$

where vector l_f contains the land fractions, vector b_{σ^2} the variance for the biosphere fluxes and vector u_{σ^2} the variance for the fossil fuel emissions for each grid cell and each week (separated into day and night time). The operator "diag" returns a diagonal matrix with the vector elements as the diagonal, which means that we assume no correlations among different fluxes. The effect of correlation length between different fluxes is investigated in Part 2 (Nickless et al., 2014). Multiplying by the land fractions guarantees that the prior uncertainties for coastal grid cells are scaled accordingly and ocean only grid cells are set to zero. This is important, because in the network design we want to focus on the reduction of uncertainty for the land fluxes only.

Observational uncertainties are set to 2 ppm for all existing and potential stations (except in one sensitivity test). Again, the uncertainties are specified in terms of their standard deviation and we assume no correlations among the uncertainties of different observations. In this way $\mathbf{C}_c$ also becomes a diagonal matrix.

3.3 Cost function

We must optimize some scalar quantity derived from the posterior covariance. Rayner et al. (1996) noted the sensitivity of the optimal network to this choice. Common options are the average uncertainty of individual fluxes (the trace of the covariance, cost function J_{Ct}) or the uncertainty of the integrated flux (the sum of all elements, cost function J_{Ce}):

$$J_{\mathrm{Ct}} = \sqrt{\sum_{i=1}^{n} C_{f_{ii}}} \tag{17}$$

$$J_{\mathrm{Ce}} = \sqrt{\sum_{i=1}^{n} \sum_{j=1}^{n} C_{f_{ij}}} \tag{18}$$

where n is the number of elements in the diagonal of matrix $\mathbf{C}_f$.

If we start the optimisation from the base network, then the transport matrix always includes the s-r relationship for our six stations in the base network (see Table 1). We can then add the s-r relationship for the three remaining existing stations and/or for the stations from the candidate list and construct $\mathbf{C}_f$. In order to find the set of stations that minimizes our cost function we apply the incremental optimization, where we add only one station at a time from the candidate list to the base network and calculate $\mathbf{C}_f$. We choose the station that gives us the smallest cost function value and add it to the network and also remove it from the candidate list. We than repeat the process until our optimal network has reached a certain maximum size or the candidate list is empty.

We assume that observations (CO_2 concentration measurements) will be available from all stations from the candidate list and the base network at an hourly time scale. The s-r relationship we calculate with LPDM therefore represents the sensitivity of hourly observations to weekly fluxes.

The most computationally demanding part of the network design is to run LPDM for all candidate stations. Running LPDM with driving data for one month takes about 2 h on a 2.9 GHz machine. However, all runs can be performed in parallel since they are all independent. Results are stored and different scenarios for the network design can be studied without the need to re-run LPDM. We evaluate the different networks in terms of the uncertainty reduction:

$$U_\mathrm{R} = 1 - \frac{\hat{J}_\mathrm{Ce}}{J_\mathrm{Ce\,prior}} \qquad (19)$$

where $\hat{J}_\mathrm{Ce}$ is the optimal cost function value and $J_\mathrm{Ce\,prior}$ the cost function value based on the prior uncertainties. Instead of $J_\mathrm{Ce\,prior}$ we could also use $J_\mathrm{Ce\,base}$ which is the cost function value for the base network.

4 Results and discussion

After running LPDM for all existing and potential stations we calculate the influence function or sensitivity matrix for each of the stations. We can also sum over the influence functions for the whole month and this provides us with the surface footprint for each station. The surface footprint shows us the area that is visible by that station. Figure 4a and b present the footprint for Cape Grim as an example for an existing station from the base network for July and January respectively. It can be seen that the area that is visible by Cape Grim differs by a large amount between the two seasons. In SH summer, Cape Grim samples mainly clean air coming from the Southern Ocean. The influence from the land is very small. However, in SH winter the dominant wind direction varies and Cape Grim is sampling air that may also be influenced by surface fluxes from the south-eastern part of Australia. The surface footprint for a potential station in Alice Springs is presented in Fig. 4c and d for both seasons. Due to its central location, a station in Alice Springs would be able to detect the influence of potential surface fluxes from a large part of the Australian continent. However, from the surface footprint alone we cannot estimate how much a station at Alice Springs would help us to reduce the uncertainties on net CO_2 fluxes.

We then use Eq. (14) to decide whether or not we have to include the boundary conditions in our inversions. We investigate existing and potential stations close to the north, south, east and west coast of Australia (i.e. Darwin, Aspendale, Arcturus and Geraldton). All diagonal elements of $\mathbf{C}_b$ turn out to be smaller than one for those stations, which means that the uncertainty contribution of the boundary concentrations to the estimates of the surface fluxes can be considered negligible. Therefore, we decided not to include the boundary concentrations in the network design process. Note, that this would change for a smaller domain or one where the large-scale concentrations were more uncertain.

In the following we present the results for the network design. We start by assessing the stations in the base network in terms of their ability to reduce the uncertainties

on net CO_2 flux estimates. We then add new stations from the candidate list to the base network using the incremental optimisation and the cost function as described in Sect. 3.3. Finally, we compare this optimal network with a network that was designed from scratch (i.e. we assume no existing stations).

4.1 Base network

Currently, there are six ground based measurement stations in Australia that measure CO_2 continuously. As discussed earlier some of these stations were designed to measure well-mixed air (i.e. Cape Grim) or background concentrations for detecting fugitive emissions (i.e. Arcturus). However, the surface footprint of Cape Grim for example indicates that our existing stations are also able to pick up the influence from the land depending on the dominant wind direction. Here, we test how useful our existing stations are in terms of estimating CO_2 fluxes from CO_2 concentration measurements. In a first experiment, we assume that all stations provide the same quality of measurements and we set the data uncertainty to 2 ppm for each station. In a second experiment, we assign a lower uncertainty to measurements from Cape Grim and a higher uncertainty to measurements from Aspendale and Wollongong.

Table 3 shows the ranking and uncertainty reduction for the first experiment for all stations in the base network for the two seasons individually and together. We use J_{Ce} as a cost function, which means that we include all elements of the posterior covariance matrix. Incremental optimization is used to determine the ranking of the stations and their overall contribution to the uncertainty reduction. We start with an empty network and then add the station which provides the greatest reduction in uncertainty. We repeat this until all six stations have been added to the network, which then forms the base network.

The results vary for the two seasons. We get a larger reduction of uncertainty in SH winter (July) than in SH summer (January) due to the difference in dominant wind direction and due to the fact that the prior biosphere flux uncertainties are also larger in July (see Fig. 2). However, for both seasons individually and together, Darwin, Wollongong,

Arcturus and Aspendale rank as the four most important stations in our base network. These stations are already able to reduce the uncertainties on CO_2 flux estimates by more than 27 %. Gunn Point and Cape Grim are the least important stations. However, this is misleading if one is only assessing the ranking as presented in Table 3. In fact,

5   Gunn Point alone provides about the same reduction in uncertainty as Darwin (12.47 % vs. 12.81 %), because these two stations are located very close together. Due to the fact that the uncertainty reduction for Darwin is slightly larger than the one obtained from Gunn Point, Darwin is added first to the network which makes Gunn Point "redundant". Cape Grim on the other hand provides the smallest reduction in uncertainty

10 even when assessed on its own in an empty network, because Cape Grim samples the "cleanest" air of all the six stations.

The ranking of the existing stations in the base network also depends on the accuracy of the measurements provided by those stations. In a sensitivity experiment, we set the the observational uncertainty for Cape Grim to 1 ppm, because this is Aus-

15 tralia's primary ground based measurement station and we expect a high accuracy for the data. We increase the observational uncertainty for Aspendale and Wollongong to 3 ppm, because these two stations are located close to large sources of fossil fuel emissions. We keep the uncertainty at 2 ppm for all remaining stations. The new ranking of the existing stations can be found in Table 4. It can be seen, that Cape Grim

20 now becomes one of the most important stations in the base network. In contrast, Aspendale and Wollongong, which were ranked high in the first experiment, become less important. This highlights the sensitivity of the network design to the observational uncertainty assigned to each station with consequences for interpreting the results from the network design.

25 The small uncertainty reduction that we achieve in SH summer suggests that the current network is not suitable for estimating biosphere fluxes for Australia for that season. Overall, the six existing ground based measurement stations are able to reduce the uncertainties on CO_2 flux estimates for Australia by nearly 30 % in both experiments

for the two seasons together. This is an interesting result, since most stations were not primarily designed to measure the contributions from land fluxes.

4.2 Extended network

We extend the base network by one station at a time using the incremental optimization for each season individually and for both seasons together. We add a total of six new stations from the candidate list and the results are presented in Table 5. The results show different network extensions for the two seasons with only one station (Moree) in common. The base network already provides a substantial reduction in flux uncertainties for the SH winter season (43 %) and the six new stations allow for a further 18 %. Stations are mainly added in the northern part of the Australian continent (see Fig. 5a). In the SH summer season, the base network can only provide an uncertainty reduction of 10 %, but with the new stations added we can achieve an additional 30 %. The six new stations are mainly added in the north-eastern part of Australia (see Fig. 5b), filling the gaps between existing stations.

If we focus on the results for the network considering both seasons together, the first four stations added to the base network are the same as for the SH summer case, although in a slightly different order. This is in agreement with the fact that new stations are able to provide a greater reduction in uncertainty for the SH summer than for the SH winter. The two additional stations (Longreach and Tennant Creek) in the extended network for both seasons are located in the central-eastern part of the country (see Fig. 5c).

Adding six new stations to the base network would lead to a doubling in the number of ground based measurement stations in Australia and we would be able to achieve a reduction on the prior uncertainties of CO_2 flux estimates of more than 50 %. It is worth pointing out, that Tumbarumba (ranked third in the optimization see Table 5) is actually not a new station from the candidate list. Tumbarumba is an established station that is currently not operational (see Table 1). Tumbarumba used to measure CO_2

Greenhouse gas network design

T. Ziehn et al.

|◀ | ▶|

◀ | ▶

Back | Close

Full Screen / Esc

Printer-friendly Version

Interactive Discussion

continuously and the network design indicates that is has great value for estimating local land fluxes.

4.3 New network

Another interesting scenario is to perform the network design by starting from an empty network (i.e. assume we do not have existing ground based measurement stations). In this way we will be able to create the most efficient network and be able to compare it with the extended network from the previous section that is based on our existing stations.

The ranking of the stations added to the network by the incremental optimisation is shown in Table 6. Again, the networks vary depending on the season due to the difference in wind direction and prior biosphere flux uncertainties, but also show some similarities. Mornington Island and Moree for example are the highest ranked stations for each season individually and combined. Only in the SH summer season Tumbarumba turns out to be even more important. Stations at Mornington Island and Moree would be able to reduce the CO_2 flux uncertainties by more than 27 % (summer and winter). In comparison with the base network, we can see that these two stations alone would be able to provide the same reduction in uncertainty as the four highest ranked existing stations (Darwin, Wollongong, Aspendale and Arcturus) together. If we wanted to achieve the same performance as the extended network consisting of 12 stations (six existing stations plus six new stations), we would only require nine stations when designing the network from scratch. The distribution of the stations in the new network (which is not based on the existing stations) does not look that much different from the extended network (see Fig. 5d–f), however the optimisation has more freedom to place stations closer to regions where prior uncertainties are largest.

4.4 Comparison with previous study

In a previous study, Law et al. (2004) found that if we wanted to erect a new measurement station in Australia it should ideally be located in the north-west or central part of the continent. This is in contrast to our results, which suggest that it would be most beneficial to add a new station in the north-eastern part of Australia. Both studies use a similar metric for the optimal network design, namely the reduction in flux uncertainty over the Australian continent, but there are also many differences in the methodology and set-up between the two studies. For example, Law et al. (2004) uses response functions for the inversion and Australia is divided into only 12 subregions for which average annual mean uncertainties are calculated. The base network in Law et al. (2004) consists of only two station (Cape Grim and Cape Ferguson). In this study the base network comprises six stations with two stations located in the north of the continent. However, even if we start the network design from the same base network as in Law et al. (2004), the first station added to the network will still be located in the north-east.

The largest impact on the difference in the new stations location might be due to the formulation of the prior flux uncertainties. In Law et al. (2004) the prior flux uncertainties are either assumed to be constant (i.e. set to $1\,\mathrm{kg\,C\,m^{-2}\,yr^{-1}}$) for all regions or variable based on the largest monthly flux for each region. In both cases, the largest prior flux uncertainties are assigned to the north-west or central part of Australia. It is therefore, not surprising, that a new station would then also be located in the same region. In our study, the prior flux uncertainties are scaled with NPP, which is obtained from high resolution simulations of a land surface model at a weekly time scale for two seasons. The largest uncertainties can be found in the north-eastern part of the continent and this is where we would add the first new station. Again, this highlights that the location chosen for new stations (or network) critically depends on the prior knowledge (i.e. prior flux uncertainties) provided.

4.5 Logistic constraints for potential stations

Potential stations in this study were selected based on existing locations of stations in the Australian Bureau of Meteorology National Radar Loop (NRL, 2014). Although this ensures that all potential sites are accessible and maintained, we cannot differen-
tiate between the sites in terms of actual costs associated in setting up the equipment to measure CO_2 concentrations. For example, some sites may require the erection of a tall tower whereas other sites may already have one that could potentially be used for additional equipment. Costs associated to maintain a certain site may also differ by a large amount due to the site's distance away from the nearest major town or air-
port or its location being offshore. It is very challenging to include all this information, which might not even be available at the time, into the cost function. Weights need to be assigned for all penalty terms and that may require tuning, which is time consum-
ing. One way to circumvent this problem would be to change a station's observational uncertainty as a proxy for logistical issues. For example, we could use a smaller obser-
vational uncertainty for a station that is easily accessible and cost efficient to run and a higher observational uncertainty for a station that is located offshore and does not provide a tall tower already. In this way the cost function does not need to be changed and we can use all available information for a potential site by changing only one quan-
tity. This will be investigated in a future study.

5 Summary and conclusions

Running a Lagrangian particle dispersion model in reverse mode provides an efficient way of obtaining the relationship between concentration observations (receptor) and ground fluxes (source). Here, we used LPDM and the Bayesian framework to obtain the transport matrix (source-receptor relationship) for existing ground based measurement stations and a list of candidate stations. An incremental optimization scheme was then used to design an optimal network of ground based measurement stations for Australia.

Title Page

Abstract | Introduction

Conclusions | References

Tables | Figures

◄ | ►

◄ | ►

Back | Close

Full Screen / Esc

Printer-friendly Version

Interactive Discussion

Existing stations were assessed and ranked in terms of their ability to reduce CO_2 flux estimates for the whole continent. New observational networks were designed based on existing stations and starting from an empty network.

We found that the influence from outside the domain (boundary concentrations) has only a small impact on the network design, and we therefore did not include uncertainties related to boundary concentrations in this study. In addition to biosphere flux uncertainties, which were derived from high resolution BIOS2 model runs, we also considered uncertainties for fossil fuel emissions. These uncertainties were derived from ten realisations from FFDAS at 0.1° resolution. However, the fossil fuel fluxes are very localized with a range of many orders of magnitude. When we aggregated those fluxes to the 1.8° resolution used for the network design, we smoothed out most of the large fluxes and their variability across the ten realisations. Consequently, the uncertainties we derived for the fossil fuel fluxes were also small so that they did not have an impact in this study. If we would perform inversions for only a small region of Australia using a much higher resolution, then the fossil fuel uncertainties would become much more important and, depending on the resolution, they might even dominate the overall surface flux uncertainties.

The assessment of existing ground based measurement stations in Australia showed that they would be able to reduce surface flux uncertainties by about 30 %, which indicates the value of making in situ measurements (taken from all wind directions) at sites that are designed primarily for baseline measurements, such as Cape Grim.

If we want to halve the uncertainties on Australian flux estimates we need to double the number of existing stations, that are currently operational. Assuming all sites give measurements of the same quality and can be modelling equally well, the two most important new stations would be located in the north (Mornington Island) and in the east (Moree) of the continent. This also shows that new stations do not necessarily need to be located far inland in order to pick up the influence from local sources. In fact, a new station at Mornington Island would be located offshore, but still be able to observe the influence from the Australian biosphere. It is also worth noting that

Tumbarumba, an existing station that is currently not operational, has great value for the estimation of local sources. In terms of costs associated with erecting a new site, it might be more efficient to put an already existing site back into operation.

Although we included logistic constraints in setting up the candidate list of stations, we did not include actual costs (i.e. to erect the station or for maintenance) in the network design. A relative measure of the ease of taking and modelling measurements at any given location can be accounted for in the network design through using a variable data uncertainty across measurement locations. This would be a valuable extension to this study, given the sensitivity found in the one test case undertaken in which data uncertainties were modified. We also plan to extend the study to optimise a network for estimating both CO_2 and CH_4 fluxes since some in-situ instruments are designed to measure both species.

References

Asefi-Najafabady, S., Rayner, P. J., Gurney, K. R., McRobert, A., Song, Y., Coltin, K., Elvidge, C., and Baugh, K.: A new global gridded dataset of CO_2 emissions from fossil fuel combustion: methodology, evaluation and analysis, J. Geophys. Res., in review, 2014. 7570

Chevallier, F., Ciais, P., Conway, T. J., Aalto, T., Anderson, B. E., Bousquet, P., Brunke, E. G., Ciattaglia, L., Esaki, Y., Fröhlich, M., Gomez, A., Gomez-Pelaez, A. J., Haszpra, L., Krummel, P. B., Langenfelds, R. L., Leuenberger, M., Machida, T., Maignan, F., Matsueda, H., Morgui, J. A., Mukai, H., Nakazawa, T., Peylin, P., Ramonet, M., Rivier, L., Sawa, Y., Schmidt, M., Steele, L. P., Vay, S. A., Vermeulen, A. T., Wofsy, S., and Worthy, D.: CO_2 surface fluxes at grid point scale estimated from a global 21 year reanalysis of atmospheric measurements, J. Geophys. Res., 115, D21307, doi:10.1029/2010JD013887, 2010. 7558, 7569

Chevallier, F., Deutscher, N. M., Conway, T. J., Ciais, P., Ciattaglia, L., Dohe, S., Fröhlich, M., Gomez-Pelaez, A. J., Griffith, D., Hase, F., Haszpra, L., Krummel, P., Kyrö, E.,

Labuschagne, C., Langenfelds, R., Machida, T., Maignan, F., Matsueda, H., Morino, I., Notholt, J., Ramonet, M., Sawa, Y., Schmidt, M., Sherlock, V., Steele, P., Strong, K., Sussmann, R., Wennberg, P., Wofsy, S., Worthy, D., Wunch, D., and Zimnoch, M.: Global CO_2 fluxes inferred from surface air-sample measurements and from TCCON retrievals of the CO_2 total column, Geophys. Res. Lett., 38, L24810, doi:10.1029/2011GL049899, 2011. 7559

Enting, I. G.: Inverse Problems in Atmospheric Constituent Transport, Cambridge Univ. Press, New York, 2002. 7562

Enting, I. G., and Mansbridge, J. V.: Seasonal sources and sinks of atmospheric CO_2: direct inversion of filtered data, Tellus B, 41, 111–126, 1989. 7558

Francey, R. J., Trudinger, C. M., van der Schoot, M., Law, R. M., Krummel, P. B., Langenfelds, R. L., Steele, P. L., Allison, C. E., Stavert, A. R., Andres, R. J., and Rodenbeck, C.: Atmospheric verification of anthropogenic CO_2 emission trends, Nature Clim. Change, 3, 520–524, 2013. 7560

GLOBALVIEW-CO_2: Cooperative Atmospheric Data Integration Project – Carbon Dioxide [CD-ROM], NOAA, Boulder, CO, 2008. 7559

Hardt, M. and Scherbaum, F.: The design of optimum networks for aftershock recordings, Geophys. J. Int, 117, 716–726, 1994. 7563

Haverd, V., Raupach, M. R., Briggs, P. R., Canadell, J. G., Isaac, P., Pickett-Heaps, C., Roxburgh, S. H., van Gorsel, E., Viscarra Rossel, R. A., and Wang, Z.: Multiple observation types reduce uncertainty in Australia's terrestrial carbon and water cycles, Biogeosciences, 10, 2011–2040, doi:10.5194/bg-10-2011-2013, 2013. 7570

Kaminski, T., Heimann, M., and Giering, R.: A coarse grid three dimensional global inverse model of the atmospheric transport, 2. Inversion of the transport of CO_2 in the 1980s, J. Geophys. Res., 104, 18555–18581, 1999. 7559

Keeling, C. D., Bacastow, R. B., Bainbridge, A. E., Ekdahl, C. A., Guenther, P. R., and Waterman, L. S.: Atmospheric carbon dioxide variations at Mauna Loa Observatory, Hawaii, Tellus, 28, 538–551, 1976. 7559

Lauvaux, T., Schuh, A. E., Uliasz, M., Richardson, S., Miles, N., Andrews, A. E., Sweeney, C., Diaz, L. I., Martins, D., Shepson, P. B., and Davis, K. J.: Constraining the CO_2 budget of the corn belt: exploring uncertainties from the assumptions in a mesoscale inverse system, Atmos. Chem. Phys., 12, 337–354, doi:10.5194/acp-12-337-2012, 2012. 7566

Printer-friendly Version

Interactive Discussion

Law, R. M., Rayner, P. J., and Wang, Y. P.: Inversion of diurnally varying synthetic CO_2: network optimization for an Australian test case, Global Biogeochem. Cy., 18, GB1044, doi:10.1029/2003GB002136, 2004. 7560, 7561, 7578

Nickless, A., Ziehn, T., Rayner, P. J., and Scholes, R. J.: Greenhouse gas network design using backward Largrangian particle dispersion modelling – Part 2: Sensitivity analysis and South African test case, Atmos. Chem. Phys., in preparation, 2014. 7561, 7566, 7570, 7571

National Meteorological and Oceanographic Centre: APS1 upgrade of the ACCESS-R Numerical Weather Prediction system, Operations Bulletin Number 98, available at: http://www.bom.gov.au/australia/charts/bulletins/apob98.pdf (last access: 18 March 2014), 2013. 7569

Patra, P. K. and Maksyutov, S.: Incremental approach to the optimal network design for CO_2 surface source inversion, Geophys. Res. Lett., 29, 1459, doi:10.1029/2001GL013943, 2001. 7560

Peylin, P., Law, R. M., Gurney, K. R., Chevallier, F., Jacobson, A. R., Maki, T., Niwa, Y., Patra, P. K., Peters, W., Rayner, P. J., Rödenbeck, C., van der Laan-Luijkx, I. T., and Zhang, X.: Global atmospheric carbon budget: results from an ensemble of atmospheric CO_2 inversions, Biogeosciences, 10, 6699–6720, doi:10.5194/bg-10-6699-2013, 2013. 7559

Rayner, P. J., Enting, I. G., and Trudinger, C. M.: Optimizing the CO_2 observing network for constraining sources and sinks, Tellus B, 48, 433–444, 1996. 7560, 7571

Rayner, P. J., Enting, I. G., Francey, R. J., and Langenfelds, R. L.: Reconstructing the recent carbon cycle from atmospheric CO_2, δ^{13}C and O_2/N_2 observations, Tellus B, 51, 213–232, 1999. 7558

Rayner, P. J., Raupach, M. R., Paget, M., Peylin, P., and Koffi, E.: A new global gridded data set of CO_2 emissions from fossil fuel combustion: mehodology and evaluation, J. Geophys. Res., 115, D19306, doi:10.1029/2009JD013439, 2010. 7570

Rayner, R. J.: Optimizing CO_2 observing networks in the presence of model error: results from TransCom 3, Atmos. Chem. Phys., 4, 413–421, doi:10.5194/acp-4-413-2004, 2004. 7560

Rödenbeck, C., Houweling, S., Gloor, M., and Heimann, M.: CO_2 flux history 1982–2001 inferred from atmospheric data using a global inversion of atmospheric transport, Atmos. Chem. Phys., 3, 1919–1964, doi:10.5194/acp-3-1919-2003, 2003. 7558

Seibert, P. and Frank, A.: Source-receptor matrix calculation with a Lagrangian particle dispersion model in backward mode, Atmos. Chem. Phys., 4, 51–63, doi:10.5194/acp-4-51-2004, 2004. 7564, 7566

Tarantola, A.: Inverse Problem Theory : Methods for Data Fitting and Model Parameter Estimation, Elsevier, Amsterdam, 1987. 7562, 7563

Uliasz, M.: Lagrangian particle modeling in mesoscale applications, in: Environmental Modelling II, Computational Mechanics Publications, Southampton, 71–102, 1994. 7564

5 Wang, Y. P., Law, R. M., and Pak, B.: A global model of carbon, nitrogen and phosphorus cycles for the terrestrial biosphere, Biogeosciences, 7, 2261–2282, doi:10.5194/bg-7-2261-2010, 2010. 7570

Bureau of Meteorology National Radar Loop: Weather Watch Radars, available at: http://www.bom.gov.au/australia/radar/ (last access: 17 March 2014), 2014. 7569, 7579

10 Wunch, D., Toon, G. C., Blavier, J.-F. L., Washenfelder, R. A., Notholt, J., Connor, B. J., Griffith, D. W. T., Sherlock, V., and Wennberg, P. O.: The Total Carbon Column Observing Network, Philos. T. R. Soc. B, 369, 2087–2112, 2011. 7559

Title Page

Abstract | Introduction

Conclusions | References

Tables | Figures

|◄ | ►|

◄ | ►

Back | Close

Full Screen / Esc

Printer-friendly Version

Interactive Discussion

Table 1. Location of existing greenhouse gas measurement stations in Australia. Stations that are currently operational and provide in situ data for CO_2 are highlighted in bold typeface.

No.	Station	Location (lat, lon)	Operation Period	CO_2 measurements
1	**Arcturus**	−23.86, 148.47	2010–present	in situ, flask
2	**Aspendale**	−38.01, 145.01	2003–present	in situ
3	Cape Ferguson	−19.30, 147.10	1991–present	flask
4	**Cape Grim**	−40.70, 144.70	1976–present	in situ, flask
5	**Darwin**	−12.42, 130.89	2005–present	in situ, total column
6	**Gunn Point**	−12.20, 131.00	2011–present	in situ, flask
7	Otway	−38.31, 142.49	2005–2012	in situ, flask, flux
8	Tumbarumba	−35.39, 148.09	2004–2008	in situ, flux
9	**Wollongong**	−34.41, 150.88	2008–present	in situ, total column

Table 2. Location of potential greenhouse gas measurement stations using the location of the Bureau of Meteorology weather watch radar stations.

No.	Station	Location (lat, lon)	No.	Station	Location (lat, lon)
10	Adelaide Airport	−34.95, 138.53	40	Lemon Tree Pass	−32.73, 152.03
11	Albany	−34.95, 117.80	41	Letterbox	−34.26, 150.87
12	Alice Springs	−23.82, 133.90	42	Longreach	−23.43, 144.29
13	Berrimah	−12.46, 130.93	43	Mackay	−21.12, 149.22
14	Bowen	−19.87, 148.08	44	Marburg	−27.61, 152.54
15	Brisbane Airport	−27.39, 153.13	45	Melbourne Laverton	−37.85, 144.75
16	Broeadmeadows	−37.69, 144.95	46	Mildura	−34.23, 142.08
17	Broome	−17.95, 122.23	47	Moree	−29.50, 149.85
18	Buckland Park	−34.62, 138.57	48	Mornington Island	−16.67, 139.17
19	Cairns Airport	−16.88, 145.75	49	Mt Gambier	−37.75, 140.78
20	Cape Range	−22.10, 114.00	50	Mt Kanighan	−25.97, 152.58
21	Captains Flat	−35.66, 149.51	51	Mt Stuart	−19.35, 146.78
22	Canarvon	−24.88, 113.67	52	Perth	−31.95, 115.84
23	Ceduna	−32.13, 133.70	53	Port Hedland	−20.38, 118.63
24	Charleville	−26.42, 146.27	54	Rockhampton	−23.38, 150.47
25	Coffs Harbour	−30.32, 153.12	55	Saddle Mtn	−16.82, 145.68
26	Dampier	−20.65, 116.69	56	Sellicks Hill	−35.33, 138.50
27	Darwin Airport	−12.42, 130.87	57	Sydney Airport	−33.93, 151.17
28	East Sale	−38.12, 147.13	58	Tennant Creek	−19.63, 134.18
29	Esperance	−33.82, 121.83	59	Tindal	−14.51, 132.45
30	Eucla	−31.68, 128.89	60	Townsville	−19.25, 146.77
31	Geraldton	−28.80, 114.70	61	Wagga	−35.17, 147.47
32	Giles	−25.03, 128.30	62	Weipa	−12.67, 141.92
33	Gladstone	−23.85, 151.27	63	West Takone	−41.18, 145.58
34	Gove	−12.28, 136.82	64	Williamtown	−32.80, 151.83
35	Grafton	−29.62, 152.97	65	Willis Island	−16.30, 149.98
36	Halls Creek	−18.23, 127.66	66	Woomera	−31.16, 136.80
37	Hobart Airport	−42.83, 147.51	67	Wyndham	−15.45, 128.12
38	Kalgoorlie	−30.79, 121.45	68	Yarrawonga	−36.03, 146.03
39	Kurnell	−34.02, 151.23			

Table 3. Ranking and uncertainty reduction (U_R) for the existing stations in the base network in terms of their ability to reduce the uncertainties on CO_2 flux estimates for two seasons (SH summer and winter) represented by January and July. The data uncertainty for all stations is set to 2 ppm. The station number is provided in brackets.

Rank	Station Jul	U_R	Station Jan	U_R	Station Jul + Jan	U_R
1	Darwin (5)	20.04 %	Aspendale (2)	3.55 %	Darwin (5)	12.81 %
2	Wollongong (9)	31.22 %	Wollongong (9)	5.97 %	Wollongong (9)	20.40 %
3	Arcturus (1)	36.42 %	Arcturus (1)	8.08 %	Aspendale (2)	24.18 %
4	Aspendale (2)	40.02 %	Darwin (5)	9.14 %	Arcturus (1)	27.53,%
5	Gunn Point (6)	41.72 %	Cape Grim (4)	9.82 %	Cape Grim (4)	28.64 %
6	Cape Grim (4)	43.07 %	Gunn Point (6)	10.29 %	Gunn Point (6)	29.66 %

Table 4. Ranking and uncertainty reduction (U_R) for the existing stations in the base network in terms of their ability to reduce the uncertainties on CO_2 flux estimates for two seasons (SH summer and winter) represented by January and July. The data uncertainty is set to 1 ppm for Cape Grim, to 3 ppm for Aspendale and Wollongong and to 2 ppm for all remaining stations. The station number is provided in brackets.

Rank	Station Jul	U_R	Station Jan	U_R	Station Jul + Jan	U_R
1	Darwin (5)	20.04 %	Cape Grim (4)	2.72 %	Darwin (5)	12.81 %
2	Cape Grim (4)	33.03 %	Arcturus (1)	5.05 %	Cape Grim (4)	21.38 %
3	Arcturus (1)	38.65 %	Aspendale (2)	6.44 %	Arcturus (1)	25.44 %
4	Wollongong (9)	40.80 %	Wollongong (9)	7.65 %	Wollongong (9)	27.17 %
5	Gunn Point (6)	42.53 %	Darwin (5)	8.71 %	Gunn Point (6)	28.28 %
6	Aspendale (2)	43.18 %	Gunn Point (6)	9.18 %	Aspendale (2)	29.21 %

Table 5. Ranking and uncertainty reduction (U_R) for the new stations added to the base network for two seasons (SH summer and winter) represented by January and July. The data uncertainty for all stations is set to 2 ppm. The station number is provided in brackets.

Rank	Station Jul	U_R	Station Jan	U_R	Station Jul + Jan	U_R
1	Longreach (42)	48.28 %	Moree (47)	17.67 %	Mornington Island (48)	35.39 %
2	Gove (34)	52.03 %	Mornington Island (48)	24.96 %	Moree (47)	40.27 %
3	Tennant Creek (58)	55.01 %	Tumbarumba (8)	31.35 %	Tumbarumba (8)	43.57 %
4	Moree (47)	57.74 %	Wyndham (67)	35.52 %	Wyndham (67)	46.79 %
5	Geraldton (31)	60.11 %	Tindal (59)	38.08 %	Longreach (42)	49.16 %
6	Townsville (60)	61.52 %	Cairns Airport (19)	40.04 %	Tennant Creek (58)	50.87 %

Table 6. Ranking and uncertainty reduction (U_R) for the new stations starting from an empty network for two seasons (SH summer and winter) represented by January and July. The data uncertainty for all stations is set to 2 ppm. The station number is provided in brackets.

| Rank	Station Jul	U_R	Station Jan	U_R	Station Jul + Jan	U_R
1	Mornington Island (48)	23.34 %	Tumbarumba (8)	9.67 %	Mornington Island (48)	17.37 %
2	Moree (47)	34.14 %	Mornington Island (48)	17.71 %	Moree (47)	27.50 %
3	Longreach (42)	40.29 %	Moree (47)	25.62 %	Yarrawonga (68)	33.87 %
4	Tennant Creek (58)	45.40 %	Wyndham (67)	30.39 %	Wyndham (67)	38.57 %
5	Melbourne Laverton (45)	49.56 %	Yarrawonga (68)	33.54 %	Charleville (24)	42.03 %
6	Charleville (24)	52.35 %	Tindal (59)	36.17 %	Captains Flat (21)	44.41 %
7	Geraldton (31)	54.53 %	Cairns Airport (19)	38.26 %	Tennant Creek (58)	46.71 %
8	Gove (34)	56.71 %	West Takone (63)	40.24 %	Cairns Airport (19)	48.59 %
9	Wollongong (9)	58.66 %	Alice Springs (12)	42.25 %	Tindal (59)	50.32 %
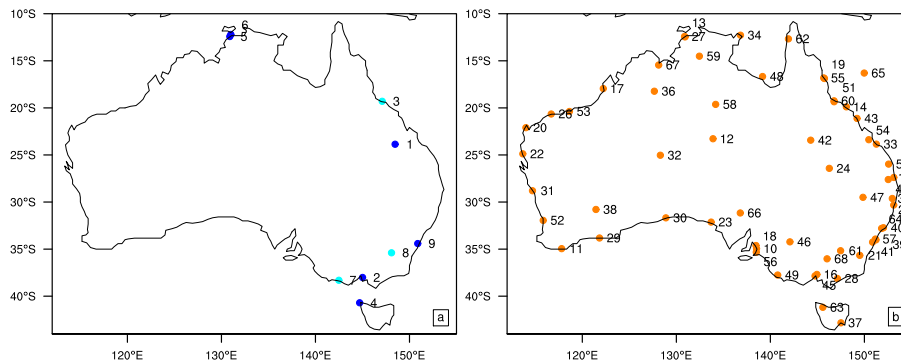
Fig. 1. Location of the existing greenhouse gas measurement stations in Australia **(a)** and potential sites using the location of the stations in the Bureau of Meteorology's National Radar Loop **(b)**. Station names are provided in Table 1 for existing sites and Table 2 for potential sites. Existing stations that are not included in the base network are marked in light blue.

Title Page

Abstract | Introduction

Conclusions | References

Tables | Figures

Back | Close

Full Screen / Esc

Printer-friendly Version

Interactive Discussion
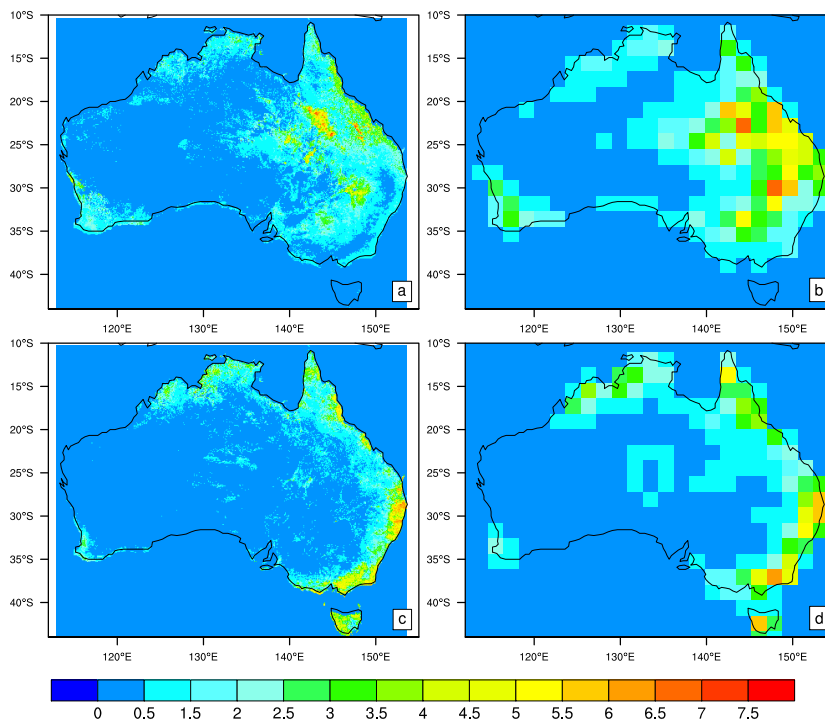
Fig. 2. Net primary productivity for 1 July **(a)** and 1 January **(c)** in $g\,C\,m^{-2}\,day^{-1}$ from BIOS2 model simulations at 0.05° resolution and derived uncertainties (one standard deviation) for the net ecosystem productivity for the first week in July **(b)** and the first week in January **(d)** in $g\,C\,m^{-2}\,week^{-1}$ at 1.8° resolution. Note that the week is devided into day and night time. One week contains 84 h day time or night time.
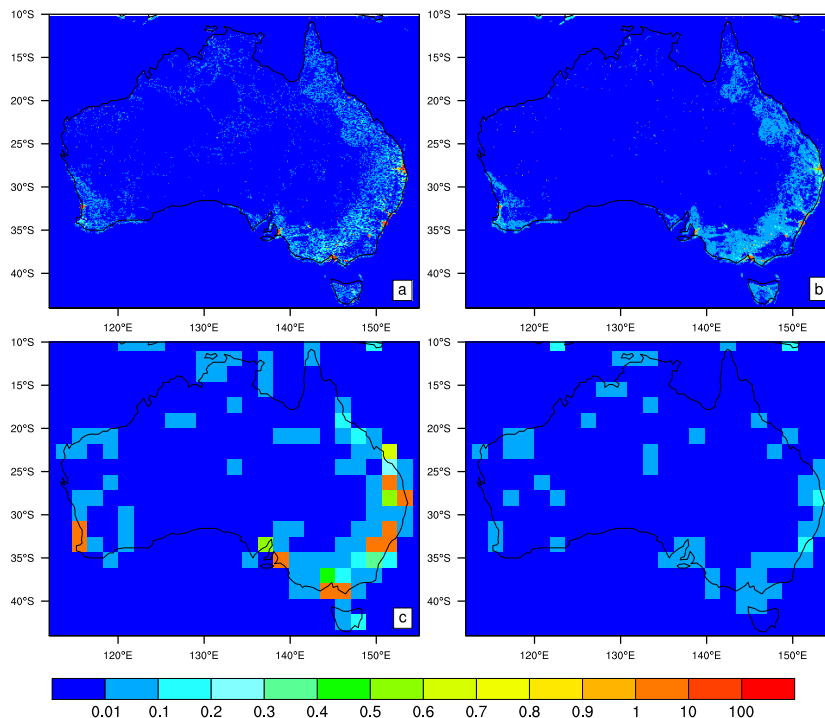
Fig. 3. One realisation of fossil fuel fluxes **(a)** as obtained from the Fossil Fuel Data Assimilations System (FFDAS) at 0.1° resolution in $gC m^{-2} week^{-1}$. Uncertainties **(b)** are calculated as one standard deviation from ten realisations. Aggregated fluxes (1.8° resolution) for one realisation are shown in **(c)** and uncertainties for the aggregated fluxes from ten realisations shown in **(d)** in $gC m^{-2} week^{-1}$. Note that the week is devided into day and night time. One week contains 84 h day time or night time.
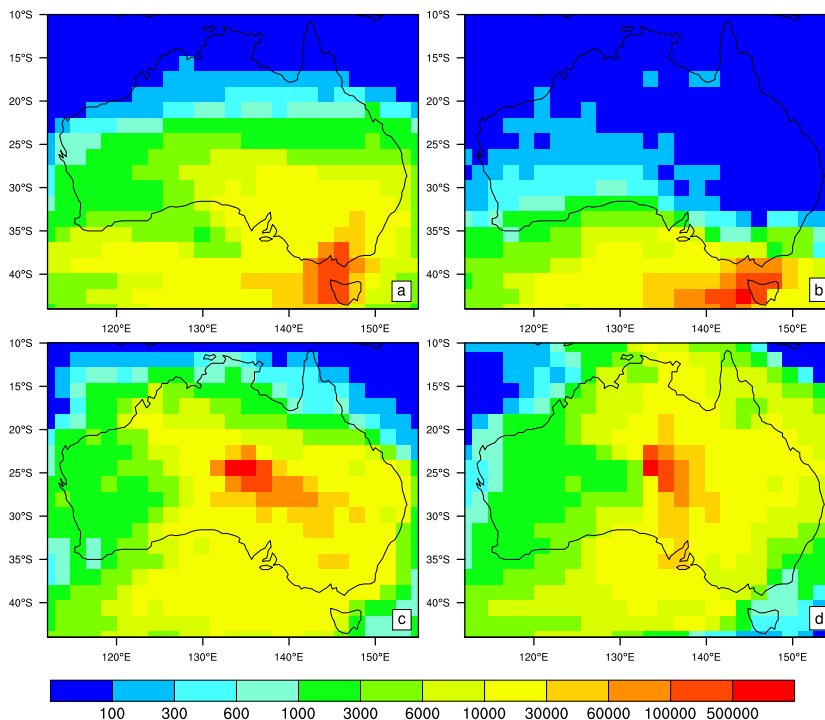
Fig. 4. Surface footprint for Cape Grim in July **(a)** and January **(b)** and for a potential station in Alice Springs in July **(c)** and January **(d)**. The footprint is the sum over the influence functions for one month and shows the number of particles that are in touch with the surface.
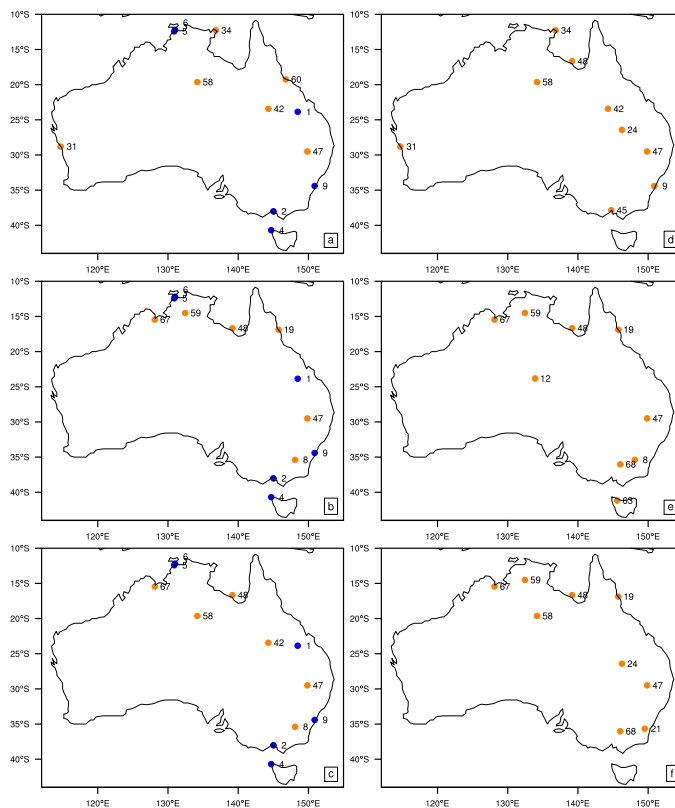
Full Screen / Esc

Fig. 5. Location of the new stations added to the base network for January **(a)**, July **(b)** and both seasons together **(c)** and location of the new stations added to an empty network for January **(d)**, July **(e)** and both seasons together **(f)**. New stations are marked with orange circles and existing stations are marked with blue circles.